Biochimica et Biophysica Acta 1858 (2016) 146–152

Contents lists available at ScienceDirect

Biochimica et Biophysica Acta

journal homepage: www.elsevier.com/locate/bbamem

A ^{2}H magic-angle spinning solid-state NMR characterisation of lipid membranes in intact bacteria

Xavier L. Warnet [a], Marwa Laadhari [b], Alexandre A. Arnold [b], Isabelle Marcotte [b], Dror E. Warschawski [a,*]

[a] UMR 7099, CNRS - Université Paris Diderot, IBPC, 13 rue Pierre et Marie Curie, F-75005 Paris, France
[b] Department of Chemistry, Université du Québec à Montréal, P.O. Box 8888, Downtown Station, Montréal, Canada, H3C 3P8

ARTICLE INFO

Article history:
Received 14 August 2015
Received in revised form 6 October 2015
Accepted 26 October 2015
Available online 28 October 2015

Keywords:
In cell solid-state nuclear magnetic resonance
Deuterium NMR
Bacteria
Lipids
Dynamics

ABSTRACT

This work proposes a new approach to characterize cell membranes in intact cells by ^{2}H solid-state nuclear magnetic resonance (NMR) in only a few hours using magic-angle spinning (MAS) and spectral moment analysis. The method was first validated on model dipalmitoylphosphatidylcholine (DPPC) membranes, allowing the detection of lipid fluctuations below the main transition temperature. Then the lipid dynamics in *Escherichia coli* membranes was compared in bacteria grown under different diets. More specifically, deuterated palmitic acid was used to isotopically label the phospholipid acyl chains in bacteria membranes, with or without the presence of protonated oleic acid. Our results showed improved lipid fluidity when bacteria were grown in the presence of oleic acid, which helps preserving the natural fatty acid profile in *E. coli* membranes. The MAS ^{2}H solid-state NMR study of membranes combined with spectral moment analysis showed to be a fast method compatible with *in vivo* bacterial studies, and should also be applicable to other micro-organisms to obtain molecular information on living cells by solid-state NMR.

1. Introduction

Since the early 2000s, nuclear magnetic resonance (NMR) has proven useful for *in-cell* structural studies of small soluble proteins [1,2]. The goal of these studies was not to determine protein structures, but rather to extract structural and dynamical information, as well as to identify potential interactions with other cellular components. Recently, two studies [3,4] showed that *in-cell* solid-state NMR (ss-NMR) could also be a powerful tool to study *membrane* proteins in their natural environment, as well as their interactions with lipids. These interactions could also be characterized by complementary experiments developed long ago, using *in-cell* solid-state NMR of lipids [5].

The first applications of static ^{2}H ss-NMR to lipids and cell membranes (*Acholeplasma laidlawii*) date back to the early 1970s [6,7] but the introduction of the 90° solid echo in 1976 improved significantly the quality of static wideline ^{2}H ss-NMR spectra [8,9] whose lineshapes are sensitive to molecular order, dynamics and therefore molecular interactions. Mutated strains of *Escherichia coli* lacking fatty acid oxidation were grown with exogenous deuterated fatty acids [10,11] until Tardy-Laporte et al. showed that it was possible to label wild-type *E. coli* membranes [12]. ^{2}H NMR order parameters and spectral moments were measured to deduce biologically-relevant structural and dynamic parameters in all sorts of synthetic and biological membranes up until today. For example, Tardy-Laporte et al. studied the effect of antimicrobial agents on cell membrane lipids, and proposed that fullerenol interacted with lipopolysaccharides of the outer membrane of *E. coli* [12].

Nevertheless, such studies, although non-invasive, can be time consuming (at least several hours to obtain a sufficient signal-to-noise ratio) which can be deleterious for some perishable samples. An approach to speed up these experiments is to combine them with magic-angle spinning (MAS). While the first combination of ^{2}H ss-NMR and MAS dates back to the late 1970s [13,14], it is only in 1986 that Clayden suggested that MAS can provide similar information to static ^{2}H ss-NMR with better sensitivity [15]. The analysis of ^{2}H MAS sideband linewidths to extract dynamic information were developed in the late 1990s [16,17] and found an important application in the case of membranes, where it has been used to probe critical fluctuations in model membranes. Indeed, Radhakrishnan and McConnell [18] predicted that these critical fluctuations would be measurable either on

Abbreviations: (MTT), 3-(4,5-dimethylthiazol-2-yl)-2,5-diphenyltetrazolium bromide; (d_{62}-DPPC), Deuterated dipalmitoyl phosphocholine; (d_{31}-PA or dC16:0), Deuterated palmitic acid; (DPPC), Dipalmitoyl phosphocholine; (DOPC), Dioleoyl phosphocholine; (DPC), Dodecyl phosphocholine; (MAS), Magic-angle spinning; (NMR), Nuclear Magnetic Resonance; (ss-NMR), Solid-state NMR; (C14:0), Myristic acid; (C15:1), Pentadecenoic acid; (PA or C16:0), Palmitic acid; (C16:1), Palmitoleic acid; (cyC17:0), Cyclopropyl heptadecanoic acid; (C18:0), Stearic acid; (OA or C18:1), Oleic acid; (C19:0), Nonadecanoic acid.

* Corresponding author at: UMR 7099, IBPC, 13 rue Pierre et Marie Curie, F-75005 Paris, France.
E-mail address: Dror.Warschawski@ibpc.fr (D.E. Warschawski).

http://dx.doi.org/10.1016/j.bbamem.2015.10.020
0005-2736/

the relaxation of ^{2}H MAS NMR spectra or on its sideband linewidths and both effects have been verified and quantified [19,20]. However, this method has not yet been applied to the study of membranes in intact cells. Therefore in this study, we assessed the advantages of using MAS *vs.* static ^{2}H NMR to study lipids within their native environment such as intact cellular membranes. More specifically, we showed how spectral moment analysis can be used to analyse spectra obtained with MAS. This approach was tested on model systems as well as on bacteria grown on different diets.

2. Material and methods

2.1. Materials

Deuterated dipalmitoyl phosphocholine (d_{62}-DPPC) and dodecyl phosphocholine (DPC) were acquired from Avanti Polar Lipids (Alabaster, AL, USA). Oleic acid (OA), deuterated palmitic acid (d_{31}-PA), deuterium-depleted water and 3-(4,5-dimethylthiazol-2-yl)-2,5-diphenyltetrazolium bromide (MTT) were purchased from Sigma Aldrich (Saint Louis, MI, USA).

All NMR experiments were performed on a solid-state Bruker Avance III-HD wide bore 400 MHz spectrometer (Milton, Ontario, Canada), operating at a frequency of 61 MHz for deuterium, with double resonance magic-angle spinning probes using either 4 mm or 1.9 mm diameter rotors.

2.2. Sample preparation

DPPC samples were prepared with a 75% hydration content by mixing 22 mg of d_{62}-DPPC with 66 mg of ^{2}H-depleted water, transferred into a 4 mm rotor, or 2.75 mg of d_{62}-DPPC with 8.25 mg of ^{2}H-depleted water, transferred into a 1.9 mm rotor.

BL21 strain *E. coli* bacteria were grown as described before [12], with 0.19 mM d_{31}-PA incorporated in the growth medium. Another culture was prepared, incorporating 0.19 mM d_{31}-PA and 0.19 mM OA. NMR experiments were carried out on fresh samples pelleted and transferred into 4 mm rotors.

2.3. Sample characterisation

Lipid profile analyses by gas phase chromatography combined with mass spectrometry, and cellular viability assays by MTT reduction were performed as described in [12].

2.4. NMR

Static spectra were obtained using the solid-echo pulse sequence [8], with a 90° pulse length of 4 μs and an interpulse delay of 40 to 60 μs. Typically, 10 k points were acquired with a dwell time of 0.5 μs (spectral width of 1 MHz) and a repetition delay of 500 ms. The number of transients accumulated were 10,000 (1.5 h) *vs.* 20,000 (3 h) for DPPC

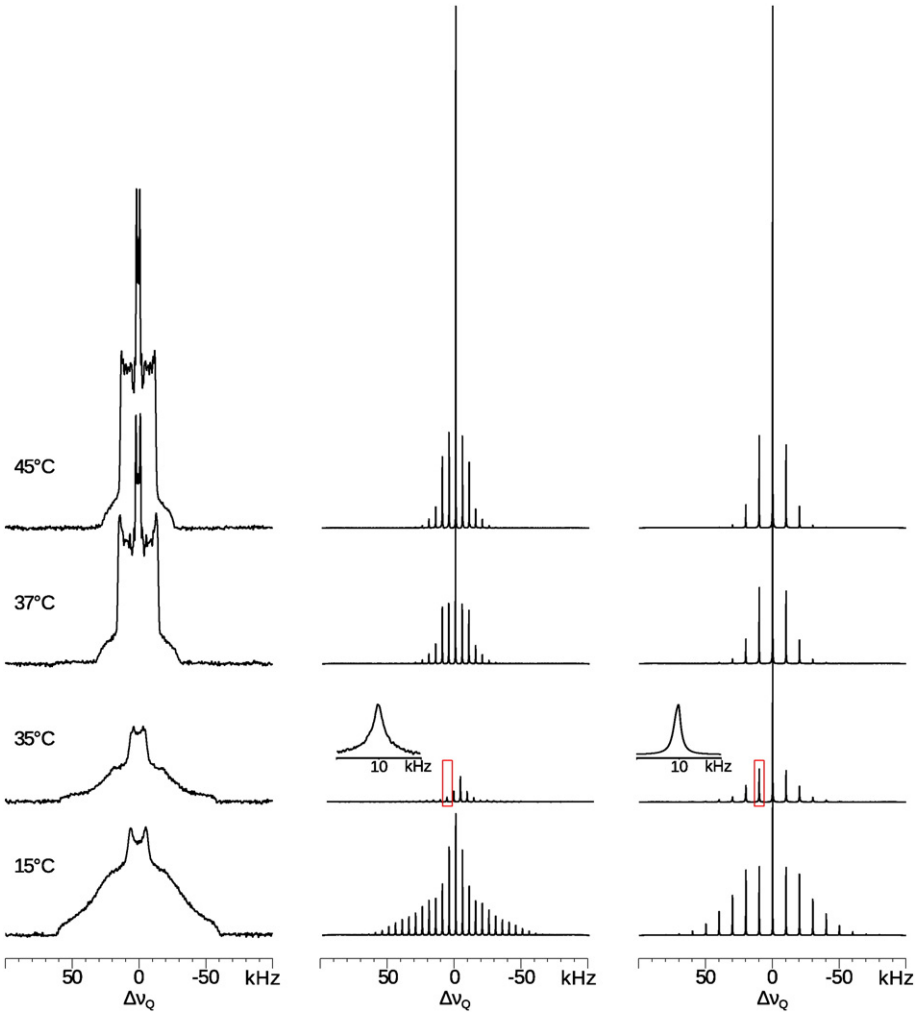

Fig. 1. Static and MAS (5 and 10 kHz) ^{2}H ss-NMR spectra of d_{62}-DPPC at 25 °C, 35 °C, 37 °C and 45 °C. Static spectra were obtained with 10 k scans. MAS spectra were obtained with 1 k scans.

and *E. coli* samples respectively. Processing was performed by using only 2000 points, left shifting by a couple of points to start from the top of the echo, automatic baseline correction and a line broadening of 20 Hz.

Spectra acquired at 5 or 10 kHz MAS frequencies were obtained using a modified Hahn-echo pulse sequence [15,21], with an initial 45° pulse and an interpulse delay equal to one rotor period (100 or 200 μs). Typically, 128 k points were acquired with a dwell time of 1 μs (spectral width of 500 kHz) and a repetition delay of 500 ms. The number of transients accumulated with MAS were 1000 (10 min) *vs.* 2000 (20 min) for DPPC *vs. E. coli* samples respectively. Processing was performed by using only 64 k points, left shifting by a couple of points to start from the top of the echo, automatic baseline correction and 20 Hz line broadening.

Experiments on model membranes were also performed on a 1.9 mm magic-angle spinning probe, at 10 or 20 kHz spinning frequency, with a 2.5 μs 90° pulse and an un-modified Hahn-echo pulse sequence. Temperature was calibrated and corrected at each spinning speed with ethylene glycol [22]. The equilibration time, in case of multi-temperature experiments, was 15 min.

2.5. Moment calculation

The second moment M_2 can be calculated using Eq. (1) [23], ν_Q being the motionless quadrupolar splitting and $<S^2_{CD}>$ the mean square order parameter.

$$M_2 = \frac{\int_0^\infty \omega^2 f(\omega) d\omega}{\int_0^\infty f(\omega) d\omega} = \frac{4\pi^2 \nu_Q^2}{5} \left\langle S_{CD}^2 \right\rangle \quad (1)$$

As shown by Maricq and Waugh [13], the spreading of the deuterium spectrum into spinning sidebands allows for a more simple way to extract spectral moments (see Eq. (2)), ω_r being the spinning rate ($\omega_r = 2\pi\upsilon r_r$, where υ_r is expressed in Hz) and A_N being the area of the Nth sideband.

$$M_2 = \omega_r^2 \frac{\sum_{N=0}^{\infty} N^2 A_N}{\sum_{N=0}^{\infty} A_N} \quad (2)$$

Spectral moments were either calculated according to Eq. (1), using the matNMR software [24], or Eq. (2), using any commercial or open source pick-picking software (Bruker Topspin or the aforementioned matNMR software) and spreadsheet application, such as LibreOffice Calc.

3. Results and discussion

The use of MAS guarantees an increase in sensitivity for solid-state NMR, which is of crucial interest for ^{2}H NMR of biological samples that are diluted and have to be studied while fresh to avoid degradation. Indeed, cellular viability assay by MTT reduction indicated a decrease of *E. coli* viability from 70% after 1 h down to 30% after 15 h, and this decrease was almost not affected by MAS (Table S1). In order to establish the feasibility of *in cell* magic-angle spinning ^{2}H NMR, the similarity and precision of the information extracted by MAS compared to the one obtained with static ^{2}H NMR had to be verified. We have therefore first studied artificial membranes made of d_{62}-DPPC (perdeuterated on their acyl chains), which behaviour is well known [23].

A side advantage of using MAS is that echoes or alternative sequences to remove the effects of deadtime and acoustic ringing [25,26] are not essential, provided signal is detected from the top of the first rotational echo, which implies signal loss at slow spinning frequencies. Using echoes in MAS is nevertheless possible, if synchronised with the rotor period, and using a 180° Hahn echo after one rotor period [20] proved beneficial for retrieving sensitivity and improving the spectral baseline. Because the radio-frequency power available on the ^{2}H channel for a standard 4 mm probe is usually insufficient for uniform excitation of a broad ^{2}H spectrum, the classical Hahn echo sequence was modified by replacing the initial 90° pulse by a 45° pulse, as suggested by Bloom and Clayden [15,21]. This results in a slight decrease in sensitivity but allows a uniform excitation profile across the whole spectrum width.

We have first verified that, as expected, sensitivity was greatly increased by MAS. A good quality spectra can thus be obtained in 15 min (see Fig. 1). While temperature was carefully calibrated and corrected at all spinning rates, we noticed that, in a 4 mm diameter rotor, the heating induced by spinning was around 2 °C at 5 kHz, and around 5 °C at 10 kHz. Increasing the rotor spinning frequency increases the sensitivity, reduces the echo time loss, but also increases the heating by friction and reduces the number of spinning sidebands from which spectral moments can be extracted. According to Eq. (2), although an infinitely fast rotation would result in no spinning sideband and no possible moment measurement, an accurate moment can be measured with only one sideband, provided its intensity is large enough. However, with a small number of sidebands, the impact of the smallest sideband to the error in moment measurement may become crucial. A compromise must be found and our experiments showed us that, provided the signal-to-noise was good enough, a few spinning sidebands were sufficient to provide accurate moment values. In practice, spinning frequencies between 5 and 20 kHz were appropriate. The gain in sensitivity in such conditions was between one and two orders of magnitude (see Figure S1 in the Supplementary Information), while the error remained below 10% with only two sidebands remaining at high temperatures (see Figure S2 in the Supplementary Information).

On Fig. 1, we observe a severe ^{2}H NMR line broadening in d_{62}-DPPC, slightly below its main phase transition temperature of 37 °C. In the static case, the reduction of signal-to-noise ratio is visible at around 35 °C (Fig. 1 and Figure S3). Under MAS, the line width of the isotropic band and of each sideband was monitored, and broadening occurred

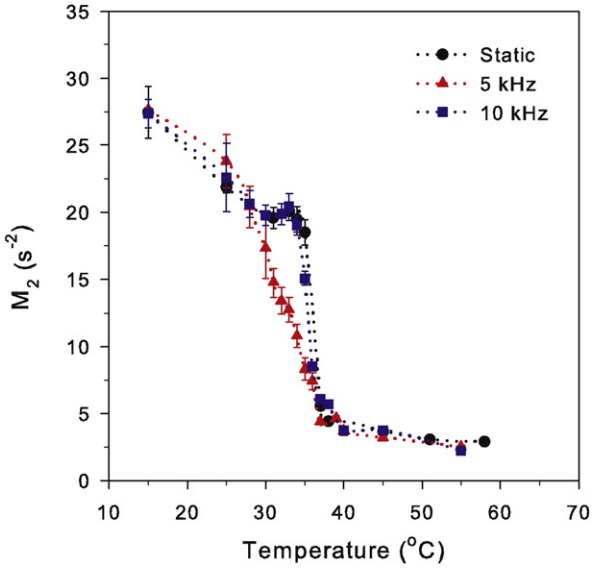

Fig. 2. Plots of M_2 from ^{2}H ss-NMR spectra of d_{62}-DPPC as a function of temperature. Eq. (1) was used for the static sample (circles). Eq. (2) was used for 5 kHz (triangles) and 10 kHz (squares) spinning.

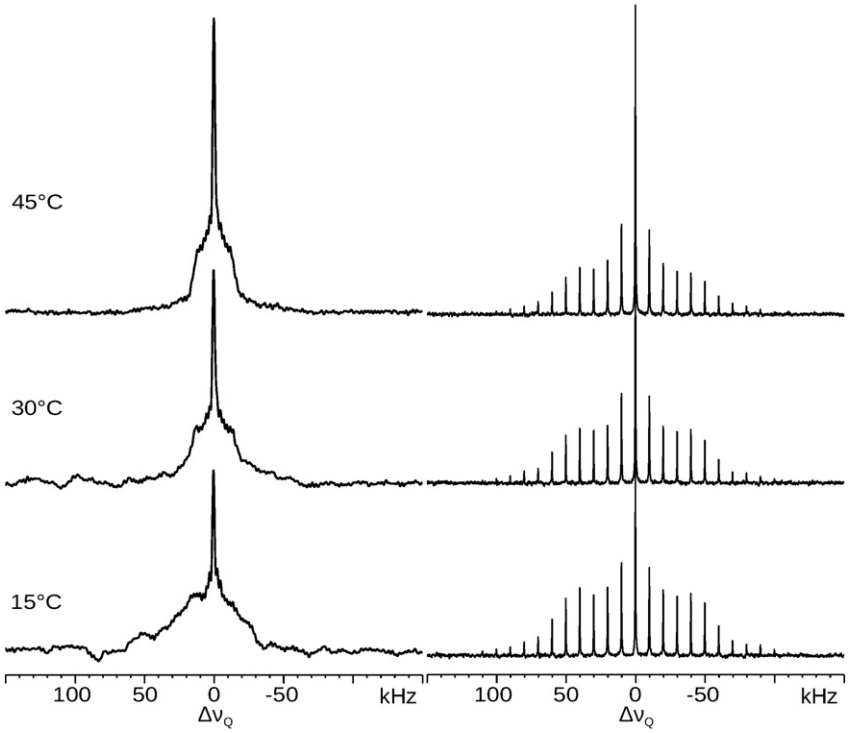

Fig. 3. Static and MAS (at 10 kHz) ^{2}H NMR spectra of *E. coli* incorporating d_{31}-PA at 15 °C, 30 °C and 45 °C. Static spectra were obtained with 20 k scans (3 h). Spinning spectra were obtained with 2 k scans (20 min).

ca. 34 °C. Since the same dynamic process seems to be responsible for broadening of static *and* spinning samples, interference of molecular motion with the rotor rotation cannot be solely responsible for such observed broadening [15,27]. Nevertheless, MAS allows for easy line width assessment and, as can be seen in Fig. 1, broadening is greater at 5 than at 10 kHz. To rule out the sole effect of the Hahn echo (longer at 5 kHz than at 10 kHz), spectra were also acquired without any echo, showing the same tendency (see Figure S4), pointing towards a low frequency dynamic process interfering with low frequency rotation of the rotor.

This type of spectral broadening has been reported in the case of critical fluctuations in DOPC/d_{62}-DPPC/cholesterol mixtures at around 29 °C,

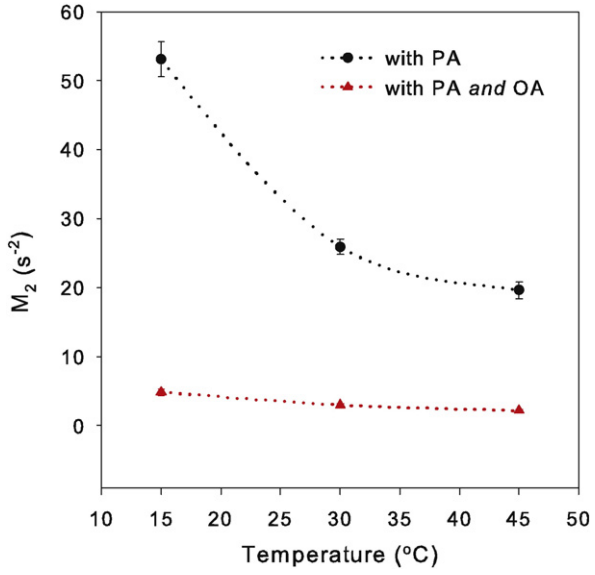

Fig. 4. Plots of M_2 from ^{2}H ss-NMR spectra of *E. coli* incorporating d_{31}-PA, with (triangles) and without (circles) protonated OA, as a function of temperature for 10 kHz spinning, using Eq. (2).

and has been assigned primarily to global lipid lateral diffusion effects [19,20,28]. Fluctuations, induced by the temporary coexistence of lipid clusters in different phases, have also been reported in simpler lipid mixtures, including local motion due to progressive acyl-chain melting in what has been called the sub-main transition region [29–31]. More work will be necessary to precisely identify the global and local molecular motion responsible for such increased relaxation and broadening.

Individual local order parameters cannot be measured when the distribution of ^{2}H labels and quadrupolar splittings is broad, as is the case with deuterated biological samples. In such cases, moment analysis is a good alternative since ^{2}H NMR spectral moments are related to the averaging of quadrupolar interactions by chain motion, as the mean order parameters would be. In particular the second moment M_2 is directly related to the mean square order parameter S^2_{CD} (see Eq. (1)), and thereby provides a convenient global picture of the state of the membrane. In d_{62}-DPPC, the static ^{2}H NMR M_2 decreases from 40×10^9 s^{-2} to 3×10^9 s^{-2} when the temperature increases from 0 °C to 50 °C, with a sharp transition at the phase transition temperature of 37 °C [23]. A similar variation is observed in bacterial membranes grown on d_{31}-PA [10,12].

Table 1
Average proportion of the major fatty acid chains in *E. coli* phospholipids under various growth conditions, determined by gas chromatography/mass spectrometry. Cyclopropane fatty acids are counted as unsaturated.

	No enrichment	With exogenous dC16:0	With exogenous dC16:0and C18:1
C14:0	2%	1%	1%
C15:1	5%	5%	0%
C16:0	39%	55% (69% deuterated)	45% (67% deuterated)
C16:1	1%	3%	6%
cyC17:0	13%	11%	14%
C18:0	2%	2%	1%
C18:1	31%	14%	23%
C19:0	2%	1%	2%
others	5%	9%	8%
Total saturated	**48%**	**60%**	**51%**
Total unsaturated	**52%**	**40%**	**49%**

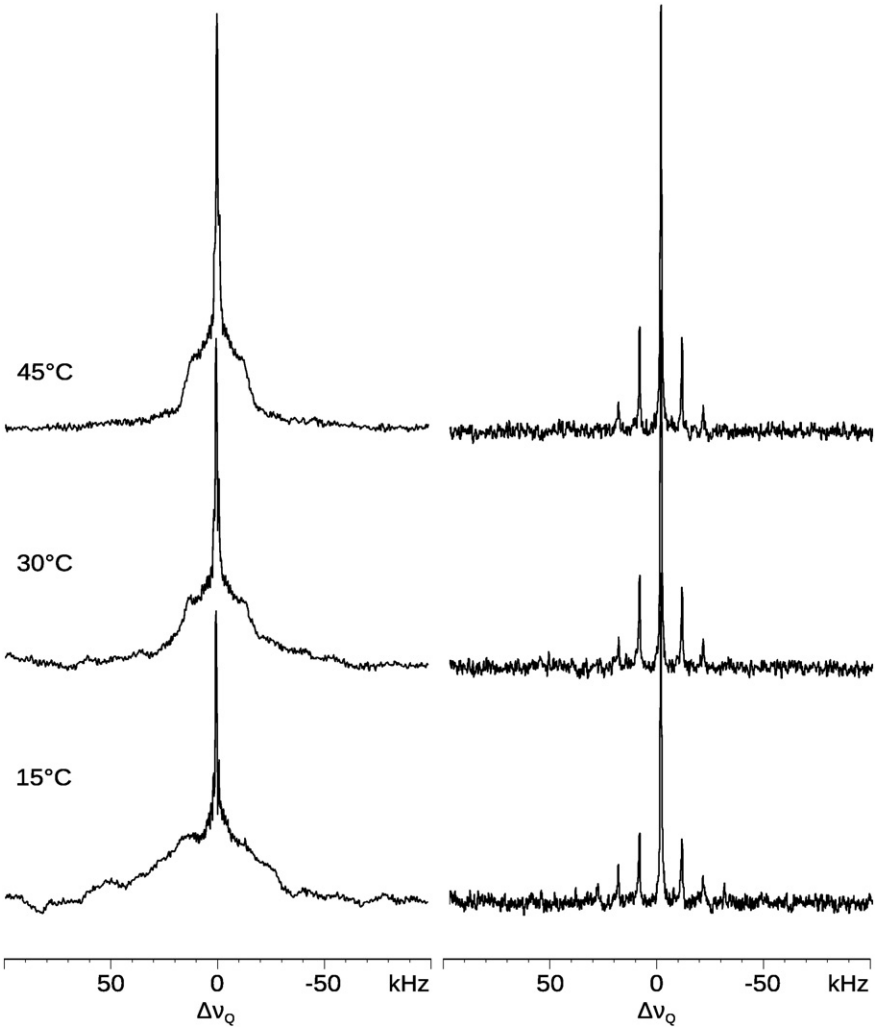

Fig. 5. Static and MAS (at 10 kHz) ^{2}H NMR spectra of *E. coli* incorporating d_{31}-PA and protonated OA at 15 °C, 30 °C and 45 °C. Static spectra were obtained with 20 k scans. Spinning spectra were obtained with 2 k scans.

Using magic angle spinning, we measured ^{2}H NMR M_2 values for d_{62}-DPPC which were identical to the same static sample and to literature values [23], at temperatures between 15 °C and 55 °C, and at spinning frequencies of 5 kHz and 10 kHz (Fig. 2). Although our static spectra could only be analysed with continuous integration (Eq. (1)), our spinning results were analysed using both the continuous integration and the simpler discrete sideband integration (Eq. (2)), with the same results, provided the number of sidebands and their intensities were sufficient (a minimum of 2 sidebands ensures an error below 10%). Although M_2 should be invariant to sample rotation [13], which is what we observe if we compare the static and the 10 kHz traces, we see a slight discrepancy at 5 kHz, between 28 and 36 °C. We believe this results from the line broadening discussed previously, which may affect the measurement of the low intensity sidebands, and in turn affect the accuracy of the measured moment. A more precise measurement could be obtained by accumulating more, thereby losing the advantage of fast acquisition. Alternatively, we have preferred spinning at 10 kHz in the rest of the article.

Once the approach was validated with DPPC membranes, we have applied ^{2}H MAS NMR to real biological cells. Our first biological sample was made of intact wild-type *E. coli* cells, incorporating d_{31}-PA (dC16:0), tested at several temperatures and at a spinning of 10 kHz (Fig. 3). A good ^{2}H signal-to-noise ratio, with a very good baseline, was obtained in twenty minutes instead of 3 h for a static spectrum. An automatic pick-picking routine was applied to the spectra, allowing for a quick and easy measurement of M_2 as a function of temperature. By probing just three different temperatures (15 °C, 30 °C, 45 °C), the membrane rigidity and its variation could be characterized in less than two hours (Fig. 4), and agreed well with known data [12]. This protocol is compatible with *in vivo* solid-state NMR studies of bacteria, as shown by our viability assays, and by other groups [32].

In our previous work [12], we have shown by gas phase chromatography that a widespread *E. coli* strain such as BL21 was able to incorporate d_{31}-PA. We have also checked that PA was the most abundant fatty acid present, and that a significant amount could be deuterated using our protocol. d_{31}-PA is therefore a good probe to reflect the behaviour of the majority of bacterial membrane lipids. Nevertheless, we have shown that incorporation of exogenous PA reduced the amount of unsaturated fatty acids in the bacterial membrane. Because this may alter the membrane rigidity or its phase transition temperature, we thus proceeded to grow wild-type *E. coli* cells with d_{31}-PA in the medium, in presence of an equal amount of protonated OA (C18:1).

Here we show by gas phase chromatography that indeed, the addition of OA mostly restores the wild-type proportion of saturated and unsaturated fatty acids, thereby probably better reflecting the natural fluidity of the bacterial membrane (Table 1). We observe here that the most abundant fatty acids are C16:0, C18:1 and cyC17:0 (cyclopropane derivative, often misassigned as C17:1 [33,34]). The samples studied here contain a very low proportion of palmitoleic acid (C16:1), in disagreement with some studies [10,12] but in agreement with others

[35]. The addition of *protonated* OA slightly reduces the amount of deuterated lipids in the sample, and hence the sensitivity of the method, but it hardly reduces the proportion of deuterated PA (around 70%) which remains the most abundant fatty acid in the membrane.

Following the protocol described above, we analysed in less than two hours the bacterial membranes grown on dC16:0 *and* C18:1 to assess the effect of OA. While an obvious effect is the reduced deuterium signal-to-noise ratio due to the increased number of protonated fatty acids, the other visible effect is a narrower distribution of quadrupolar splittings indicating a lower rigidity (Fig. 5). This effect was confirmed by the extracted M_2 values (Fig. 4) indicating that *E. coli* grown only on PA was mostly in the gel phase, with a higher proportion of fluid phase as the temperature was raised, whereas *E. coli* grown on both palmitic *and* oleic acids was always in the fluid phase, as expected for most wild-type bacteria [36].

4. Conclusions and perspectives

Lipids constitute half the weight of biological membranes and their structural diversity signals a variety of functions that is worth exploring [37]. We have herein established a new approach to characterize membrane lipids in intact cells in a few hours, thus reducing the possibility of sample degradation and allowing for *in vivo* studies of bacteria. This protocol combines ^{2}H solid-state NMR, magic-angle spinning and spectral moment analysis, and it was first validated on model membranes, allowing the detection of molecular fluctuations below the main phase transition temperature. We have extended this method to *E. coli* bacteria grown on deuterated palmitic acid, with or without the presence of protonated oleic acid, showing that membrane fluidity was related to the diet that the bacteria were grown on.

We anticipate that our approach will prove valuable in providing information regarding other diet-induced changes, lipid-protein interactions or membrane curvature, helping to characterise membranes that are not as well known, for example of algae, fungi or worms grown on different fatty acids [38–40]. Thereby, solid-state NMR is exploring yet a new frontier of structural biology by tackling *in-cell* (in some cases even *in vivo*) biomolecular studies, strengthening the link between molecular structure, dynamics and function [41–42].

Transparency document

The Transparency document associated with this article can be found, in the online version.

Acknowledgements

This work was supported by the CNRS (UMR 7099), the Université Paris Diderot, the Labex Dynamo (ANR-11-LABX-0011-01), and the Natural Science and Engineering Research Council (NSERC) of Canada. The French Ministère de l'Enseignement Supérieur et de la Recherche and the Canadian Groupe de Recherche Axé sur la Structure des Protéines (GRASP) are acknowledged for the award of scholarships to X.L.W and M.L., respectively. We would like to thank Mathieu Babin for the gas phase mass spectrometry, and Prof. Jim ^{2}H. Davis for helpful discussions.

Appendix A. Supplementary data

Supplementary data includes cellular viability assays (Table S1) and ^{2}H NMR sensitivity, error and line width measurements as a function of spinning rate and temperature (Fig. S1, S2, S3 and S4). Supplementary data associated with this article can be found in the online version, at http://dx.doi.org/10.1016/j.bbamem.2015.10.020.

References

[1] Z. Serber, A.T. Keatinge-Clay, R. Ledwidge, A.E. Kelly, S.M. Miller, V. Dötsch, High-resolution macromolecular NMR spectroscopy inside living cells, J. Am. Chem. Soc. 123 (2001) 2446–2447.
[2] A.Y. Maldonado, D.S. Burz, A. Shekhtman, In-cell NMR spectroscopy, Prog. Nucl. Magn. Reson. Spectrosc. 59 (2011) 197–212.
[3] R. Fu, X. Wang, C. Li, A.N. Santiago-Miranda, G.J. Pielak, F. Tian, In situ structural characterization of a recombinant protein in native Escherichia coli membranes with solid-state magic-angle-spinning NMR, J. Am. Chem. Soc. 133 (2011) 12370–12373.
[4] M. Renault, R. Tommassen-van Boxtel, M.P. Bos, J.A. Post, J. Tommassen, M. Baldus, Cellular solid-state nuclear magnetic resonance spectroscopy, Proc. Natl. Acad. Sci. U. S. A. 109 (2012) 4863–4868.
[5] R.E. Jacobs, E. Oldfield, NMR of membranes, Prog. Nucl. Magn. Reson. Spectrosc. 14 (1981) 113–136.
[6] E. Oldfield, D. Chapman, W. Derbyshire, Deuteron resonance – novel approach to study of hydrocarbon chain mobility in membrane systems, FEBS Lett. 16 (1971) 102–104.
[7] E. Oldfield, D. Chapman, W. Derbyshire, Lipid mobility in acholeplasma membranes using deuteron magnetic resonance, Chem. Phys. Lipids 9 (1972) 69–81.
[8] J.H. Davis, K.R. Jeffrey, M. Bloom, M.I. Valic, T.P. Higgs, Quadrupolar echo deuteron magnetic resonance spectroscopy in ordered hydrocarbon chains, Chem. Phys. Lett. 42 (1976) 390–394.
[9] G.W. Stockton, K.G. Johnson, K.W. Butler, A.P. Tulloch, Y. Boulanger, I.C.P. Smith, J.H. Davis, M. Bloom, Deuterium NMR study of lipid organization in acholeplasma laidlawii membranes, Nature 269 (1977) 267–268.
[10] J.H. Davis, C.P. Nichol, G. Weeks, M. Bloom, Study of the cytoplasmic and outer membranes of Escherichia coli by deuterium magnetic resonance, Biochemistry 18 (1979) 2103–2112.
[11] J. Pius, M.R. Morrow, V. Booth, ^{2}H solid-state NMR investigation of whole Escherichia coli interacting with antimicrobial peptide MSI-78, Biochemistry 51 (2012) 118–125.
[12] C. Tardy-Laporte, A.A. Arnold, B. Genard, R. Gastineau, M. Morancais, J.L. Mouget, R. Tremblay, I. Marcotte, A H-2 solid-state NMR study of the effect of antimicrobial agents on intact Escherichia coli without mutating, Biochim. Biophys. Acta 1828 (2013) 614–622.
[13] M.M. Maricq, J.S. Waugh, NMR in rotating solids, J. Chem. Phys. 70 (1979) 3300–3316.
[14] J.L. Ackerman, R. Eckman, A. Pines, Experimental results on deuterium NMR in the solid-state by magic angle spinning, Chem. Phys. 42 (1979) 423–428.
[15] N.J. Clayden, Computer simulations of H-2 MAS NMR spinning side band spectra, Chem. Phys. Lett. 131 (1986) 517–521.
[16] M.J. Duer, C. Stourton, H-2 double-quantum NMR spectroscopy for the study of molecular motion in solids, J. Magn. Reson. 129 (1997) 44–52.
[17] M. Cutajar, S.E. Ashbrook, S. Wimperis, H-2 double-quantum MAS NMR spectroscopy as a probe of dynamics on the microsecond timescale in solids, Chem. Phys. Lett. 423 (2006) 276–281.
[18] A. Radhakrishnan, H. McConnell, Composition fluctuations, chemical exchange, and nuclear relaxation in membranes containing cholesterol, J. Chem. Phys. 126 (2007) 185101.
[19] S.L. Veatch, O. Soubias, S.L. Keller, K. Gawrisch, Critical fluctuations in domain-forming lipid mixtures, Proc. Natl. Acad. Sci. U. S. A. 104 (2007) 17650–17655.
[20] J.H. Davis, L. Ziani, M.L. Schmidt, Critical fluctuations in DOPC/DPPC-d(62)/cholesterol mixtures: H-2 magnetic resonance and relaxation, J. Chem. Phys. 139 (2013) 045104.
[21] M. Bloom, J.H. Davis, M.I. Valic, Spectral distortion effects due to finite pulse widths in deuterium nuclear magnetic resonance spectroscopy, Can. J. Phys. 58 (1980) 1510–1517.
[22] D.S. Raiford, C.L. Fisk, E.D. Becker, Calibration of methanol and ethylene-glycol nuclear magnetic resonance thermometers, Anal. Chem. 51 (1979) 2050–2051.
[23] J.H. Davis, Deuterium magnetic resonance study of the gel and liquid-crystalline phases of dipalmitoyl phosphatidylcholine, Biophys. J. 27 (1979) 339–358.
[24] J.D. van Beek, matNMR: a flexible toolbox for processing, analyzing and visualizing magnetic resonance data in Matlab®, J. Magn. Reson. 187 (2007) 19–26.
[25] C. Jaeger, F. Hemmann, EASY: a simple tool for simultaneously removing background, deadtime and acoustic ringing in quantitative NMR spectroscopy–part I: basic principle and applications, Solid State Nucl. Magn. Reson. 57-58 (2014) 22–28.
[26] C. Jaeger, F. Hemmann, EASY: a simple tool for simultaneously removing background, deadtime and acoustic ringing in quantitative NMR spectroscopy. Part II: improved ringing suppression, application to quadrupolar nuclei, cross polarisation and 2D NMR, Solid State Nucl. Magn. Reson. 63-64 (2014) 13–19.
[27] D. Suwelack, W.P. Rothwell, J.S. Waugh, Slow molecular motion detected in the NMR spectra of rotating solids, J. Chem. Phys. 73 (1980) 2559–2569.
[28] J.R. Banigan, A. Gayen, N.J. Traaseth, Correlating lipid bilayer fluidity with sensitivity and resolution of polytopic membrane protein spectra by solid-state NMR spectroscopy, Biochim. Biophys. Acta 1848 (2015) 334–341.
[29] D. Papahadjopoulos, K. Jacobson, S. Nir, T. Isac, Phase transitions in phospholipid vesicles. Fluorescence polarization and permeability measurements concerning the effect of temperature and cholesterol, Biochim. Biophys. Acta 311 (1973) 330–348.
[30] L. Cruzeiro-Hansson, J.H. Ipsen, O.G. Mouritsen, Intrinsic molecules in lipid membranes change the lipid-domain interfacial area: cholesterol at domain interfaces, Biochim. Biophys. Acta 979 (1989) 166–176.
[31] M. Nielsen, L. Miao, J.H. Ipsen, K. Jørgensen, M.J. Zuckermann, O.G. Mouritsen, Model of a sub-main transition in phospholipid bilayers, Biochim. Biophys. Acta 1283 (1996) 170–176.
[32] G. Zandomeneghi, K. Ilg, M. Aebi, B.H. Meier, On-cell MAS NMR: physiological clues from living cells, J. Am. Chem. Soc. 134 (2012) 17513–17519.

[33] D.F. Silbert, F. Ruch, P.R. Vagelos, Fatty acid replacements in a fatty acid auxotroph of Escherichia coli, J. Bacteriol. 95 (1968) 1658–1665.
[34] D. Oursel, C. Loutelier-Bourhis, N. Orange, S. Chevalier, V. Norris, C.M. Lange, Lipid composition of membranes of Escherichia coli by liquid chromatography/tandem mass spectrometry using negative electrospray ionization, Rapid Commun. Mass Spectrom. 21 (2007) 1721–1728.
[35] R.D. Mavis, P.R. Vagelos, The effect of phospholipid fatty acid composition on membranous enzymes in Escherichia coli, J. Biol. Chem. 247 (1972) 652–659.
[36] S. Morein, A. Andersson, L. Rilfors, G. Lindblom, Wild-type Escherichia coli cells regulate the membrane lipid composition in a "window" between gel and non-lamellar structures, J. Biol. Chem. 271 (1996) 6801–6809.
[37] G. van Meer, D.R. Voelker, G.W. Feigenson, Membrane lipids: where they are and how they behave, Nat. Rev. Mol. Cell Biol. 9 (2008) 112–124.
[38] R.T. Branca, W.S. Warren, In vivo NMR detection of diet-induced changes in adipose tissue composition, J. Lipid Res. 52 (2011) 833–839.
[39] J.A. Muller, R.P. Ross, W.F. Sybesma, G.F. Fitzgerald, C. Stanton, Modification of the technical properties of lactobacillus johnsonii NCC 533 by supplementing the growth medium with unsaturated fatty acids, Appl. Environ. Microbiol. 77 (2011) 6889–6898.
[40] M.L. Deline, T.L. Vrablik, J.L. Watts, Dietary supplementation of polyunsaturated fatty acids in Caenorhabditis elegans, J. Vis. Exp. 81 (2013), e50879.
[41] V. Sarou-Kanian, N. Joudiou, F. Louat, M. Yon, F. Szeremeta, S. Même, D. Massiot, M. Decoville, F. Fayon, J.-C. Beloeil, Metabolite localization in living drosophila using high resolution magic angle spinning NMR, Sci. Rep. 5 (2015) 9872.
[42] A.J. Simpson, Y. Liaghati, B. Fortier-McGill, R. Soong, M. Akhter, Perspective: in vivo NMR - a potentially powerful tool for environmental research, Magn. Reson. Chem. 53 (2015) 686–690.

Supplementary Information for :

A ^{2}H magic-angle spinning solid-state NMR characterisation of lipid membranes in intact bacteria

Xavier Warnet, Marwa Laadhari, Alexandre Arnold, Isabelle Marcotte and Dror Warschawski

Biochimica Biophysica Acta

Cellular viability as a function of spinning rate and time

Table S1: Percentage of surviving *E. coli* bacteria grown with exogenous protonated palmitic acid, with or without spinning at 10 kHz, determined by MTT reduction activity.

time	static samples	spinning samples
1h	70 +/- 10 %	67 +/- 4 %
3h	53 +/- 12 %	51 +/- 6 %
15h	40 +/- 7 %	31 +/- 5 %

Sensitivity as a function of spinning rate and temperature

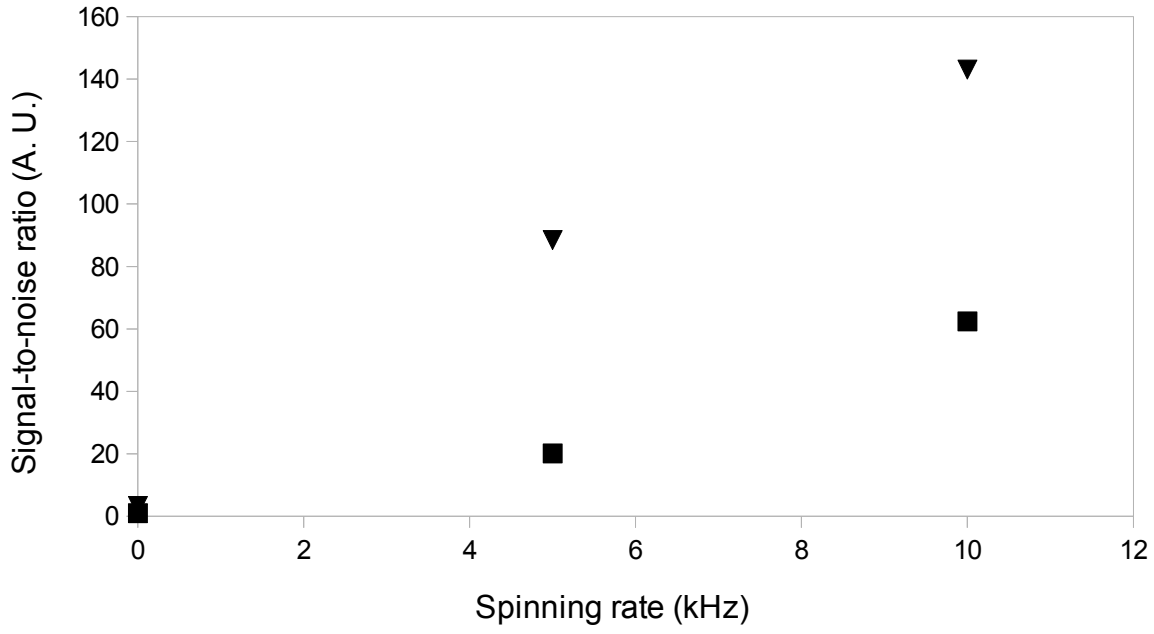

Figure S1. Signal-to-noise ratio of the whole ^{2}H spectrum of d_{62}-DPPC at 25°C (squares) and 45°C (triangles), at various spinning rates (the first, static, point at 25°C is given a sensitivity of 1).

Error as a function of spinning rate and temperature

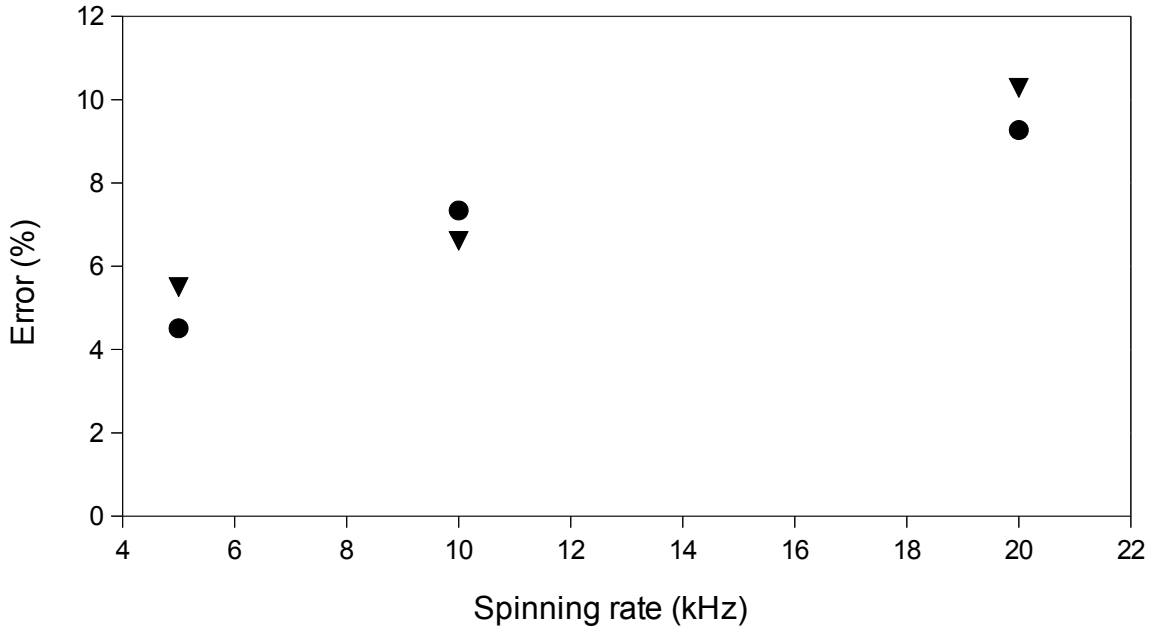

Figure S2. Error on the measurement of M_2 from ^2H spectrum of d_{62}-DPPC at 45°C (triangles) and 55°C (circles), at various spinning rates.

Sensitivity of static spectra as a function of temperature

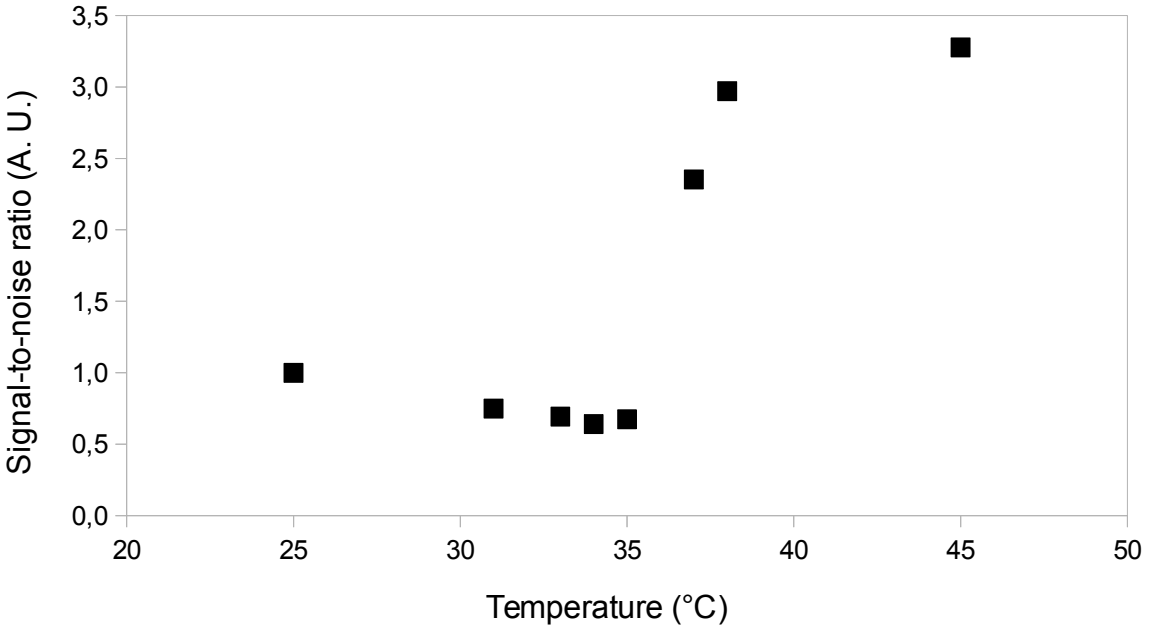

Figure S3. Signal-to-noise ratio of the whole static ^2H spectra of d_{62}-DPPC as a function of temperature (the first point at 25°C is given a sensitivity of 1).

^{2}H line broadening as a function of spinning rate and temperature

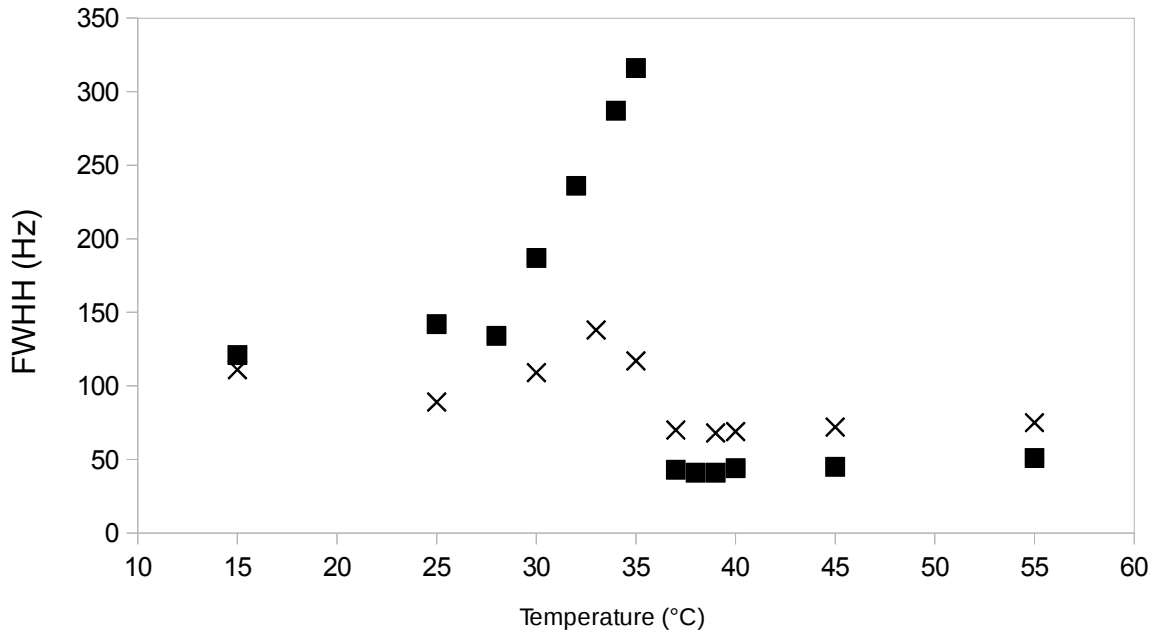

Figure S4. Line width (FWHH) measurement as a function of temperature for the central ^{2}H band of d_{62}-DPPC at a spinning rate of 5 kHz (squares) and 10 kHz (crosses), acquired with no echo.